A Benchmark Case for Structural Intensity Calculations

Christian Adams, Joachim Bös, Tobias Melz
TU Darmstadt, System Reliability, Adaptive Structures, and Machine Acoustics SAM, 64289 Darmstadt
Email: adams@sam.tu-darmstadt.de.de

Introduction

The structural intensity (STI) describes the propagation of structure-borne sound in vibrating structures from an energy source to an energy sink. Current research shows that STI analyses can be used to optimize the vibroacoustic behavior of noise radiating structures [1, 2]. The STI can either be obtained from measurements or from a finite element (FE) analysis with a subsequent STI calculation. Although the STI has been investigated for many years, it is hardly applied in vibroacoustic engineering today. One reason is the absence of a general reference to validate STI calculations and measurements. Therefore, this paper proposes a benchmark case for STI calculations. The benchmark case will be provided via the benchmark case platform of the European Acoustics Association (EAA). Thus, this benchmark case follows the instructions reported in [3]. First, this paper introduces the general procedure of STI calculations. Second, the benchmark case will be described. In the third step, a parameter study is proposed to provide reference results that can be used by other researchers for validation purposes.

STI calculation

Figure 1 illustrates the general procedure of an STI calculation from an FE analysis. During the model set-up the geometry is modeled and an energy source as well as an energy sink needs to be defined. Since STI calculations are computationally expensive, they are usually performed in the frequency domain. Thus, it is assumed that the system vibrates in steady state. Furthermore, only the STI at the structure's natural frequencies is computed. In order to find the natural frequencies a modal analysis is performed. From a subsequent harmonic analysis at the natural frequencies all necessary quantities can be obtained to calculate the STI.

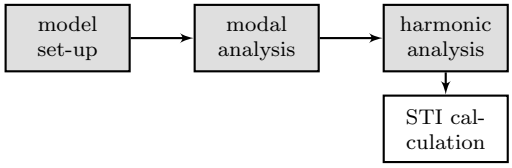

Figure 1: calculation scheme of the STI, steps of the FE analysis in gray

The STI in general is defined in analogy to the sound intensity. According to [4] the STI $\underline{\mathbf{I}}_S(f)$ in the frequency domain yields

$$\underline{\mathbf{I}}_S(f) = -\frac{1}{2}\underline{\mathbf{S}}(f)\underline{\mathbf{v}}^*(f), \tag{1}$$

where $\underline{\mathbf{S}}$ and $\underline{\mathbf{v}}^*$ denote the complex mechanical stress tensor and the conjugate complex velocities, respectively. Since many vibroacoustic problems deal with the noise radiated from vibrating shell structures, the STI $\underline{\mathbf{I}}'_S$ of shell structures can be calculated from the internal forces and moments

$$\begin{aligned}\underline{\mathbf{I}}'_S(f) = -\frac{1}{2}\Big[\; & \underline{N}_x\underline{v}_x^* + \underline{N}_{xy}\underline{v}_y^* + \underline{M}_x\underline{\dot{\phi}}_y^* \dots \\ & \underline{N}_y\underline{v}_y^* + \underline{N}_{yx}\underline{v}_x^* - \underline{M}_y\underline{\dot{\phi}}_x^* \dots \\ \dots & - \underline{M}_{xy}\underline{\dot{\phi}}_x^* + \underline{Q}_x\underline{v}_z^* \\ \dots & + \underline{M}_{yx}\underline{\dot{\phi}}_y^* + \underline{Q}_y\underline{v}_z^* \;\Big],\end{aligned} \tag{2}$$

where $\underline{\dot{\phi}}^*$ denote the conjugate complex rotational velocities [5]. The section forces and moments are defined as illustrated in Fig. 2. In Eq. (2) the prime indicates that the STI is integrated along the shell thickness. This notation, however, is common in STI literature although the prime often refers to a derivative. The contributions $\underline{N}_x\underline{v}_x^* + \underline{N}_{xy}\underline{v}_y^*$ and $\underline{N}_y\underline{v}_y^* + \underline{N}_{yx}\underline{v}_x^*$ in Eq. (2) describe the structure borne sound waves that propagate in longitudinal direction (in-plane), whereas $\underline{M}_x\underline{\dot{\phi}}_y^* - \underline{M}_{xy}\underline{\dot{\phi}}_x^* + \underline{Q}_x\underline{v}_z^*$ and $\underline{M}_y\underline{\dot{\phi}}_x^* + \underline{M}_{yx}\underline{\dot{\phi}}_y^* + \underline{Q}_y\underline{v}_z^*$ describe the structure-borne sound waves that propagate in transversal direction (out-of-plane). It should be noted that the definition of in-plane and out-of-plane waves is limited to the STI of shell structures. The real part of the STI describes the propagation of structure borne sound energy and is referred to as *active STI*

$$\mathbf{I}_{S,a}(f) = \Re\left\{\underline{\mathbf{I}}_S(f)\right\}, \tag{3}$$

whereas the imaginary part is the *reactive STI*

$$\mathbf{I}_{S,r}(f) = \Im\left\{\underline{\mathbf{I}}_S(f)\right\}. \tag{4}$$

A local maximum of the reactive STI indicates a location with maximum kinetic energy, whereas minima are located at maxima of potential energy [8].

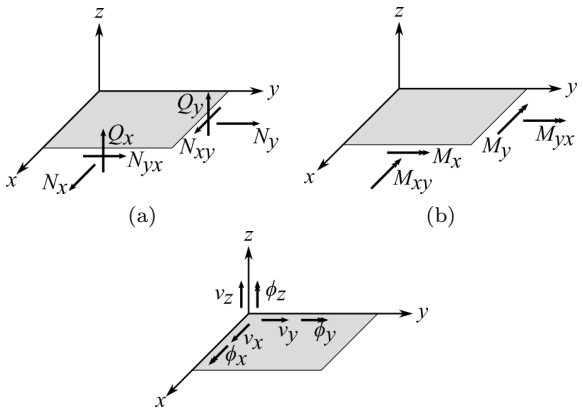

Figure 2: definition of (a) the internal forces, (b) the internal moments, and (c) the translational and rotational velocities

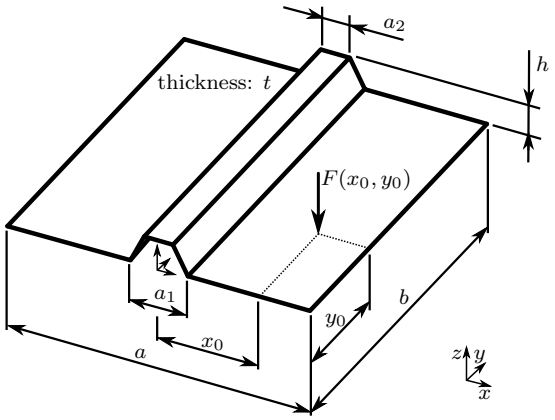

Figure 3: model of the generic car undercarriage

Table 1: geometry parameters of the generic car undercarriage

parameter	value in mm	parameter	value in mm
a	1350	h	130
a_1	258	t	5
a_2	130	x_0	500
b	1470	y_0	500

Table 2: material properties of the generic car undercarriage

property	nomenclature	value	unit
Young's modulus	E	$70 \cdot 10^9$	$\mathrm{N/m^2}$
Poisson's ratio	μ	0.33	–
mass density	ρ	2700	$\mathrm{kg/m^3}$
material loss factor	η	0.005	–

The generic car undercarriage as a benchmark case

According to [3] a benchmark case is described by (1) the geometry and propagation medium, (2) a source and a receiver, (3) the boundary conditions, (4) the differential equation that is solved, and (5) the quantity that is computed. From the scope of this paper it is clear that the latter is the STI as already introduced in Eq. (2). The points (1) through (4) are subsequently described.

The mechanical structure incorporated in this benchmark case is the generic car undercarriage illustrated in Figure 3 with the geometry parameters and material properties listed in Table 1 and 2, respectively. The structure has a rectangular shape with a trapezoidal tunnel to surround the transmission shaft. The car undercarriage is generic, i.e., simplified, but still a typical mechanical structure where STI analyses are performed, since such an automotive structure is subject to vibroacoustic analyses and optimization procedures. The source of structure borne sound energy and, thus, noise is a harmonic point force with the amplitude $\hat{F} = 1\,\mathrm{N}$ acting at the position (x_0, y_0). The energy sink (or receiver) is the radiated noise of the structure. The radiated noise is estimated by the equivalent radiated power (ERP) defined as

$$P_{\mathrm{ERP}}(f) = \frac{1}{2}\rho c \int_S \Re\left\{\underline{\mathbf{v}}_n(f)\underline{\mathbf{v}}_n^*(f)\right\} \mathrm{d}S, \tag{5}$$

where ρ denotes the air density, c the speed of sound in air, S the area of the vibrating surface, and n denotes the normal direction.

Three different boundary conditions are applied to the outer edges of the undercarriage: (1) fixed, i.e., translational and rotational displacements are set to zero, (2) simply supported, i.e., only translational displacements are set to zero, and (3) free, i.e., neither translational nor rotational displacements are restrained. Since the STI analysis of the undercarriage requires an FE analysis (see Fig. 1), the governing equation of the problem is the well-known vibration differential equation

$$\left(\mathbf{K} - \Omega^2\mathbf{M} + i\Omega\mathbf{B}\right)\mathbf{u} = \mathbf{F}, \tag{6}$$

where $\mathbf{K}$, $\mathbf{M}$, $\mathbf{B}$, and $\mathbf{F}$ denote the stiffness matrix, the mass matrix, the damping matrix, and the load vector, respectively. $\mathbf{u}$ is the vector of displacements and Ω is the angular frequency. According to [6] the damping matrix yields

$$\mathbf{B} = \frac{1}{\Omega}\eta\mathbf{K}, \tag{7}$$

since a constant material loss factor is used (see Table 2). Setting $\mathbf{B} = 0$ and $\mathbf{F} = 0$, the well-known eigenvalue problem of the undamped system is obtained

$$\left(\mathbf{K} - \omega^2\mathbf{M}\right)\tilde{\mathbf{u}} = 0, \tag{8}$$

with the natural angular frequencies ω and the mode shapes $\tilde{\mathbf{u}}$. In order to calculate the first N natural frequencies, a Block Lanczos eigenvalue extraction is used to solve Eq. (8). Considering each natural frequency as excitation frequency of the harmonic analysis, Eq. (6) is solved by a sparse solver. Table 3 summarizes the benchmark case and categorizes it according to [3].

Table 3: summary of the benchmark case

name	car undercarriage
categories	bounded 3D radiation frequency domain
equations	Eqs. (8), (6), and (2)
geometry	Figure 3
boundary conditions	outer edges fixed outer edges simply supported outer edges free
source	harmonic force $\hat{F} = 1\,\mathrm{N}$ at $x_0 = 500\,\mathrm{mm}$ and $y_0 = 500\,\mathrm{mm}$
receiver	ERP, Eq. (5)
quantity	STI, Eq. (2)

Parameter study

Since this parameter study will provide reference results for validation purposes, each step of the entire STI calculation procedure (see Figure 1) needs to be validated. This requires a large amount of data to be analyzed. Thus, this paper focuses on the most important results. For the full set of the results the reader is referred to the online resource [7].

The FE model of the undercarriage is set-up according to Figure 1 with the different boundary conditions listed in Table 3. A structured mesh of shell elements with quadratic shape functions is used. The elements' sizes are 25 mm to ensure approx. 20 elements per flexural wavelength for the first $N = 25$ natural frequencies. Table 4 lists the natural frequencies f_n calculated from the modal analysis. It should be noted that double natural frequencies occur, e.g., f_1 and f_2, f_3 and f_4, etc. of the undercarriage with fixed and simple support. The corresponding mode shapes are equal in their number of antinodes, but the phase relation between the antinodes differs, see Fig. 4. In order to validate the results of the harmonic analysis the ERP is calculated according to Eq. (5). Figure 5 illustrates the level of the ERP at the first 25 natural frequencies.

The real part and the imaginary part of the STI are illustrated in Fig. 6 for the simply supported undercarriage at the natural frequency $f_{17} = 249.13\,\mathrm{Hz}$. The maximum of the real part is located at the excitation position. Figure 7 illustrates the out-of-plane and in-plane parts of the STI. The out-of-plane STI qualitatively matches the real part of the STI (see Fig. 6), since the excitation force acts in global z-direction, thus, mainly exciting out-of-plane waves. At the transmission tunnel the out-of-plane waves turn into in-plane waves. Figure 8 illustrates the STI for the free boundary condition at $f_1 = 8.65\,\mathrm{Hz}$. Maxmima of the STI are found not only at the excitation position, but also at the outer edges of the transmission tunnel. However, this is rather a numerical error than a physical phenomenon, since the kinetic energy is non-zero at the edges due to the free boundary condition. This causes an increased imaginary part of the in-plane waves, see Figure 9.

Table 4: natural frequencies in Hz of the undercarriage for the investigated boundary conditions

n	**fixed**	**simple**	**free**	n	**fixed**	**simple**	**free**
1	86.99	60.84	8.65	14	253.79	208.40	101.96
2	87.01	61.04	12.18	15	280.38	233.94	104.85
3	102.81	75.58	18.69	16	281.42	234.80	104.97
4	103.12	75.79	28.77	17	289.77	249.13	105.21
5	130.49	101.20	28.84	18	289.86	249.21	110.76
6	130.77	101.41	36.90	19	307.78	271.46	110.80
7	171.06	138.69	41.46	20	319.66	272.08	124.65
8	171.26	138.85	45.17	21	320.43	307.11	124.86
9	224.29	188.05	46.47	22	367.13	320.23	134.32
10	224.43	188.17	50.50	23	367.19	320.71	134.77
11	231.14	188.92	50.69	24	370.79	321.77	169.10
12	235.01	191.01	80.82	25	371.37	321.82	169.42
13	252.39	207.38	80.98				

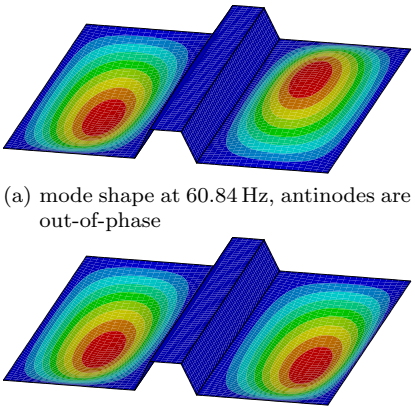

(a) mode shape at 60.84 Hz, antinodes are out-of-phase

(b) mode shape at 61.04 Hz, antinodes are in-phase

Figure 4: the first two mode shapes of the simply supported undercarriage

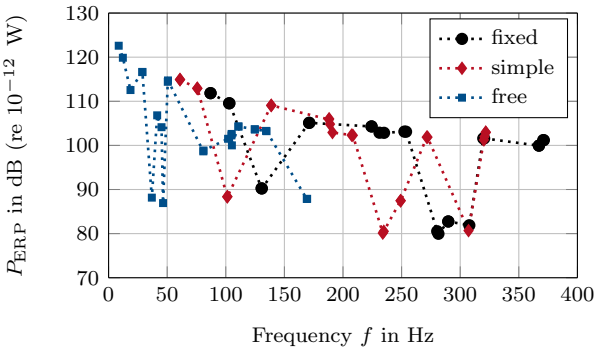

Figure 5: ERP at the natural frequencies of the undercarriage for the investigated boundary conditions

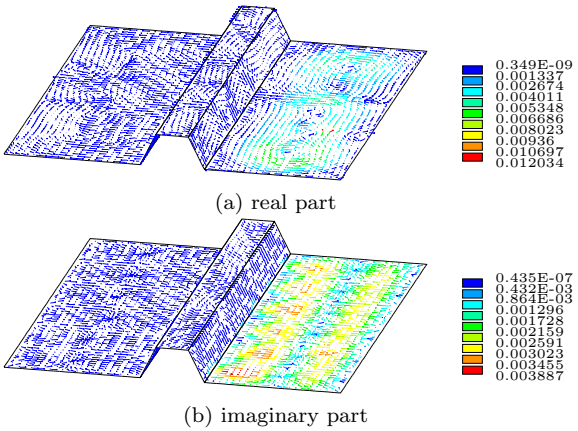

(a) real part

(b) imaginary part

Figure 6: STI in W/m at $f_{17} = 249.13\,\text{Hz}$ for the simply supported undercarriage

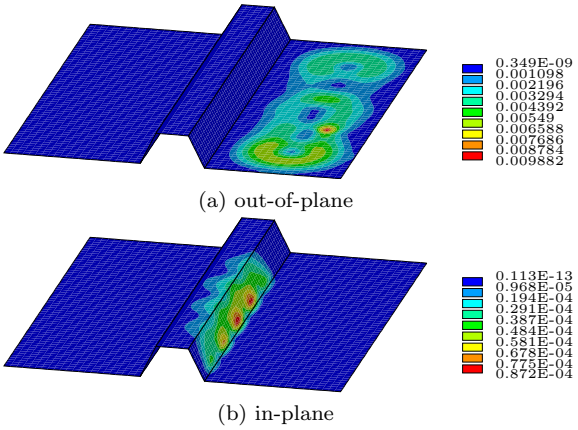

(a) out-of-plane

(b) in-plane

Figure 7: out-of-plane and in-plane STI (real part) in W/m at $f_{17} = 249.13\,\text{Hz}$ for the simply supported undercarriage

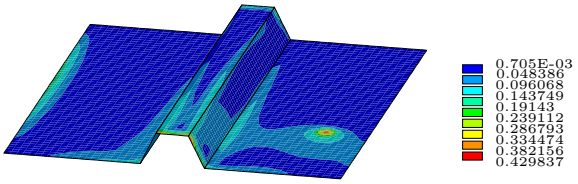

Figure 8: active STI in W/m at $f_1 = 8.65\,\text{Hz}$ for the free boundary condition

Summary

This paper proposes a generic car undercarriage as a benchmark case that allows for validating STI calculation schemes. Each step of the entire STI calculation procedure can be validated, since a full set of results will be provided online, see [7]. Before the benchmark case is submitted to the EAA, the influence of the load type (force on FE node or pressure on FE element) and the influence of the symmetry on the STI will be investigated. An experimental validation of STI calculations will be part of current research activities.

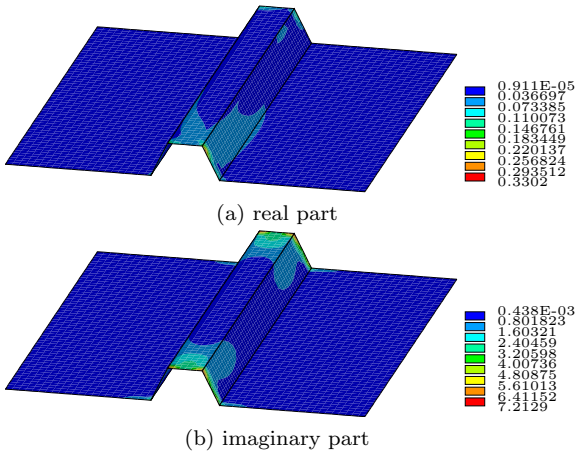

(a) real part

(b) imaginary part

Figure 9: in-plane STI in W/m at $f_1 = 8.65\,\text{Hz}$ for the free boundary condition

References

[1] Adams, C., Schaal, C., Bös, J., Melz, T.: Numerical investigation of the sound power and of the structural intensity of a permanent magnet synchronous machine. Inter-Noise 2015, San Francisco, California, USA

[2] Schaal, C., Ebert, J., Bös, J., Melz, T.: Relation between structural intensity-based scalars and sound radiation using the example of plate-rib models. Journal of Vibration and Acoustics 138 (2016), 041011-1–041011-9

[3] Hornikx, M., Kaltenbacher, M., Marburg, S.: A platform for benchmark cases in computational acoustics. Acta Acustica united with Acustica 101(2015), 811–820

[4] Hanselka, H. and Bös, J.: Maschinenakustik (Machine Acoustics), Dubbel – Taschenbuch für den Maschinenbau (Dubbel – Handbook of Mechanical Engineering), 24th ed., Springer, Berlin, 2014

[5] Romano, A., Abraham, P., Williams, E.: A poynting vector formulation for thin shells and plates, and its application to structural intensity analysis and source localization. Part I: Theory. Journal of the Acoustical Society of America, 87(3), 1990, 1166–1176.

[6] SAS Inc.: ANSYS Documentation – Theory Reference – Release 15.0, Canonsburg, 2013

[7] Adams, C., Bös, J., Melz, T.: A Benchmark Case for Structural Intensity Calculations. Research Gate project. URL: https://www.researchgate.net/project/A-Benchmark-Case-for-Structural-Intensity-Calculations, 2017

[8] Maysenhölder, W.: Körperschallenergie – Grundlagen zur Berechnung von Energiedichten und Intensitäten (Structure borne sound energy – Fundamentals of the calculation of energy densities and intensities), S. Hirzel, Stuttgart, 1994